

Catalytic performance of silica-aluminas synthesised with the help of chitosan biopolymer

Marisa Falco^a, Jaime Retuert^b, Alexis Hidrobo^b, Cristian Covarrubias^b, Paulo Araya^b, Ulises Sedran^{a,*}

^a Instituto de Investigaciones en Catálisis y Petroquímica INCAPE (FIQ, UNL-CONICET), Santiago del Estero 2654, (3000) Santa Fe, Argentina

^b Departamento de Ingeniería Química y Biotecnología, Facultad de Cs. Físicas y Matemáticas, Universidad de Chile, Beaucheff 861, Santiago, Chile

ARTICLE INFO

Article history:

Received 5 May 2009

Received in revised form 6 July 2009

Accepted 8 July 2009

Available online 16 July 2009

Keywords:

Silica-alumina

Chitosan

FCC

ABSTRACT

Mesoporous amorphous silica-aluminas were synthesised with standard aluminium and silicon sources by means of the formation of inorganic–organic composites with the addition of chitosan biopolymer, and compared to analogous catalysts synthesised conventionally. Some catalysts were subjected to hydrothermal treatment. The resulting specific surface areas were from 480 to 573 m²/g in the untreated samples and 300–430 m²/g in the hydrotreated catalysts, average pore sizes ranging from 32 to 100 Å with sharp, unimodal distributions. The chitosan materials showed higher specific surface areas and larger pore sizes than those of their non-chitosan counterparts. The most important differences in the acidic properties were in the relationships between tetrahedral and octahedral aluminium atoms, the chitosan materials having higher relative amounts of tetrahedral aluminium than the conventional silica-aluminas. Evidences of stabilization in the physical and chemical properties were observed in the chitosan-containing catalysts. The catalytic performance was evaluated with the conversion of triisopropylbenzene at 400 °C, to assess activity and accessibility, and cyclohexene at 300 °C, to assess hydrogen transfer properties. The highest activity and accessibility was observed in the hydrotreated, chitosan-containing catalyst, while hydrogen transfer capabilities were similar to those of medium unit cell sizes, equilibrium commercial FCC catalysts.

© 2009 Elsevier B.V. All rights reserved.

1. Introduction

Modern refineries are following new trends in response to the increasing demands to process heavier crudes and residual feedstocks, to control contaminants in products and emissions, and to maximize the yields of light olefins, petrochemical raw materials [1]. Consequently, the main refining processes, such as the catalytic cracking of hydrocarbons (FCC), aimed at the conversion of low value, heavy hydrocarbon feedstocks into lighter, more valuable products such as liquefied petroleum gases, gasoline and diesel fuels, are also impacted significantly. It is also a consequence that the formulation of FCC catalysts is shifting to high accessibility, resid or bottoms upgrading catalysts with active matrices and specific additives [2]. The matrix in a FCC catalyst plays a key role in providing the proper particle size and shape for the circulation of the catalyst particles in the unit [3,4], a heat sink to transport combustion heat from the regenerator to the reactor, and as good a contact as possible between the reactant hydrocarbon molecules and the main catalyst component, the Y

zeolite. Matrices can be either inactive or active, in this case supplying a pre-cracking activity for the very large molecules in the feedstock that cannot diffuse directly into the zeolite structure [5].

One of the most common active matrices of the FCC catalysts is amorphous silica-alumina, activity and coke yield enhancing with the alumina content. Silica-alumina with 13 wt% Al₂O₃ is conventionally used as a FCC catalyst active matrix [6]. The synergetic effects of HY-zeolite and silica-alumina as the two major components of a FCC catalyst, on the activity and coking tendency in the cracking of 1,3,5 tri-isopropylbenzene were studied by Hosseinpour et al. [7]. The stabilizing role of a silica-alumina matrix on the zeolite was investigated by Kubicek et al. [8], who focused on zeolite beta.

A crucial property in the FCC catalyst matrix is the distribution of their pore sizes, which must favour mass transfer processes. Since the control of the pore size distribution in various porous materials can be achieved by means of the synthesis procedure, new techniques with that aim are of interest, and the resulting materials could find commercial application. There has been a growing interest during the last years in the synthesis of mesoporous materials with controlled morphology, with pore sizes between 20 and 200 Å. One of the approaches for obtaining

* Corresponding author. Tel.: +54 342 452 8062; fax: +54 342 453 1068.

E-mail address: usedran@fiq.unl.edu.ar (U. Sedran).

these materials is the production of composites between inorganic networks, such as silica, and polystyrene, polyacrilates, and certain organic polymers such as cellulose [9,10,11]. After the removal of the organic component by calcination at different temperatures, these composites develop porosity. This approach, together with the use of biopolymers, could be employed in the synthesis of silica-aluminas [12], and Puchol et al. [13] showed that chitosan promoted silica growth under biomimetic conditions.

Chitosan, or poly- β -(1-4)-2-amino-2-deoxy-D-glucose, is the deacetylated product of the alkali treatment of chitin, an abundant, relatively low-cost biopolymer contained in the shells of crustaceans [14]. The porogenic capacity of chitosan was shown in previous works with titania or silica as the inorganic component in the composites [14,15], and the synthesis of mesoporous aluminas was achieved by Fajardo et al. [16] under a similar approach.

Commercial feedstocks in FCC, usually vacuum gas oils and residual streams from various refining processes, are extremely complex [17]. Then, test reactions become a powerful laboratory tool to evaluate the properties of new materials in relation to FCC issues [18]. Particularly, the test conversion of 1,3,5-triisopropylbenzene (TIPB, [19]) may contribute to assess accessibility properties in a potential matrix material, while that of cyclohexene (CYC6=) may help in understanding the hydrogen transfer behaviour of a catalyst. The latter reactions have a strong impact on the product distribution and the resulting quality of the fuel products, as well as on the catalyst stability [20].

It is the objective of this work to report the synthesis of mesoporous silica-aluminas with the addition of chitosan in the inorganic-organic composite, as compared to an analogous method without chitosan, which could be used as matrices in FCC catalysts. The catalytic performance of these materials was evaluated by means of the conversion of both TIPB and CYC6= in a CREC Riser Simulator laboratory reactor.

2. Experimental

2.1. Catalyst synthesis

Mesoporous silica-aluminas were synthesised using tetraethylorthosilicate (TEOS, 98%, Aldrich) and aluminium nitrate nonahydrate ($\text{Al}(\text{NO}_3)_3 \cdot 9\text{H}_2\text{O}$, 98.5%, Merck) as silicon and aluminium sources, respectively, in a two-step procedure. In the first-step a gel was obtained by precipitation: 30 g of aluminium nitrate were dissolved in 20 g of distilled water and drops of HNO_3 solution (2 N) were added under stirring until pH 1 was obtained. Afterward, 13.6 mL of TEOS was added drop by drop under stirring in 1 h to obtain Solution 1. Finally an ammonia solution (25%, Merck) was added drop by drop up to pH 10 to reach the precipitation condition. The precipitated gel was filtered and left overnight at room temperature, washed with distilled water and finally with ethanol. In the second-step the material obtained was separated in two fractions. Fraction B was calcined at 550 °C during 12 h in order to stabilize the structure of the solid. Fraction B(TH) was subjected to a hydrothermal treatment in autoclave at 150 °C during 24 h; then, it was filtered, washed with distilled water until reaching pH 7, left overnight at room temperature and finally calcined at 550 °C during 12 h. A second set of samples incorporated chitosan (1% solution of chitosan in formic acid (Solution 2)) in the first-step, previous to the addition of the ammonia solution; Solution 2 was slowly added to Solution 1 and the final mix was stirred for 1 h. Then two fractions were separated that followed the same treatments as described above: fractions Q (calcined only) and Q(TH) (calcined after the hydrothermal treatment). The resulting $\text{SiO}_2/\text{Al}_2\text{O}_3$ molar ratio in all the synthesis mixtures was 1.75.

2.2. Catalyst characterization

Catalyst physical properties and pore size distributions were assessed from the nitrogen adsorption isotherms at 77 K (desorption branch) in a Micromeritics ASAP 2010 sorption meter. The relation between tetrahedral and octahedral sites was determined by using ^{27}Al Magic-Angle-Spinning NMR (MAS-NMR) spectroscopy. ^{27}Al MAS-NMR spectra were collected on a Bruker ASX 300 spectrometer operating at a resonance frequency of 300 MHz. The quantification of Al tetrahedral atoms was done by using zeolite NaA as a reference (Al atoms only in tetrahedral coordination, peak at 52 ppm).

Total acidity was measured using a potentiometric method of titration with n-butylamine [21]. 0.05 mL of n-butylamine (0.1 N) was added to a dispersion of 0.15 g of silica-alumina in 90 mL of acetonitrile. This system was kept under steady stirring for 3 h. The suspension was then titrated using base solution volumes of 0.05 mL each time. The time elapsed before making a potential measurement was 2 min. The electrode potential variation (mV) was measured with a Hanna PH211 digital pH/mV meter. The maximum acid strength of the first titrated acid surface sites was taken to be the initial electrode potential. The total number of acid sites was estimated from the total amount of base added to reach the plateau in the potential vs. base volume curve.

The types of acid sites were identified by FTIR analysis of pyridine-sorbed on the silica-alumina samples. Briefly, the analysis was carried out as follows: the silica-alumina samples were pressed into self-supported wafers (12,000 lb/in.²), set in a Pyrex glass cell with NaCl windows and pretreated at ultra-high vacuum (10^{-6} Torr) at 300 °C for 2 h. Pyridine adsorption was carried out at 120 °C for 30 min, and then the sample was placed under ultra-high vacuum at the same temperature for 15 min in order to minimize the amount of physisorbed pyridine. The FTIR spectra of the various samples were recorded at room temperature.

2.3. Catalytic performance

The evaluation of the catalytic performances of the various samples was carried out in a laboratory CREC Riser Simulator reactor [22]. The unit has a turbine on top of a chamber that holds the catalyst bed between porous metal plates. The turbine rotates at 7500 rpm, inducing a low pressure area in the upper central zone in the reactor that makes gases recirculate in the upwards direction through the chamber and fluidize the catalyst bed. When the reactor is at the desired experimental conditions, the reactant is fed with a syringe through an injection port and vaporizes instantly, thus setting the initial time. After the desired reaction time is reached, the gaseous mixture is evacuated immediately and products can be sent to analysis. Additional descriptive details can be found in, e.g., [23,24]. The experiments of conversion of 1,3,5-triisopropylbenzene (TIPB, Fluka 97%) were conducted at 400 °C, with a mass of catalyst of 0.4 g, catalyst to oil relationship (C/O) of 2.35 and reaction times of 4, 6, 8 and 10 s. The experiments of conversion of cyclohexene (CYC6=, Merck > 99%) were conducted at 300 °C, with a mass of catalyst of 0.2 g, catalyst to oil relationship (C/O) of 1.17 and reaction times of 4, 6, 8 and 10 s. Mass balances closed to more than about 94% in all the cases.

Reaction products were analyzed by on-line capillary gas chromatography. In the case of TIPB reactant, a 30 m length, 250 μm i.d. and 0.25 μm dimethyl polysiloxane phase thickness column was used. In the case of CYC6= reactant, a 60 m length, 200 μm i.d. and 0.50 μm dimethyl silicone phase thickness column was used. Coke on the catalyst was determined by means of a temperature programmed oxidation procedure; carbon oxides from the combustion of coke were transformed into methane and quantified with the help of a FID detector.

Table 1
Physical properties of the silica-aluminas.

Catalyst	Specific surface area (m ² /g)	Average pore size (Å)
B	487	32
B(TH)	296	66
Q	573	50
Q(TH)	433	100

3. Results and discussion

The silica-aluminas obtained were all amorphous materials, as confirmed by XRD analysis, their physical properties being shown in Table 1. In general, the specific surface areas of the different catalysts are large, but the samples that incorporated chitosan in their preparation, both with and without the intermediate hydrothermal treatment, have higher specific surface areas than the corresponding reference samples. It is interesting to observe in Fig. 1 that the resulting pore size distributions are all unimodal and can be considered sharp. Moreover, it can be seen that the samples with chitosan have average pore sizes larger than those of the reference samples, and that the treated samples B(TH) and Q(TH) have average pore sizes larger than those of the base materials B and Q, respectively. These evidences suggest that the pore size in these materials could be controlled in the synthesis.

The acidic properties of the various samples are shown in Table 2. The acid strength as inferred from the first reading in the potentiometric titration with n-butyl amine is higher in the base catalysts B and Q than in the related, hydrothermally treated samples. It is observed that the decline produced by the treatment is more important in the samples prepared without chitosan. The number of acid sites is also higher in the base catalysts B and Q, but

the loss produced by the hydrothermal treatment is similar in both cases (with and without chitosan).

In order to identify the types of acid sites existing in the silica-alumina catalysts, the FTIR analysis of pyridine-sorbed silica-alumina samples was carried out (see Fig. 2). In the FTIR spectra the band at 1548 cm⁻¹ corresponds to the pyridinium ion formed by interaction between pyridine and Brønsted acid sites, whereas the band at 1444 cm⁻¹ is ascribed to the coordination of pyridine molecules with Lewis acid sites. The third strong band around 1490 cm⁻¹ has been attributed to a contribution of both Brønsted and Lewis acid sites [25]. According to the FTIR spectra there exist both Lewis and Brønsted sites on the catalysts, the amount of Lewis sites being about 4.5 times that of Brønsted sites in the base catalysts B and Q, as assessed from the intensity of the corresponding Brønsted and Lewis bands (refer to Table 2). However, the hydrothermally treated samples showed a significant relative increase in the number of Lewis sites. This predominant concentration of Lewis acid sites found in the various catalysts is consistent with the well-known acid characteristics of typical silica-aluminas [26,27].

The ²⁷Al MAS-NMR spectra showed that the Al atoms in the silica-aluminas are in two different coordination environments: tetrahedral and octahedral, as indicated by the peaks at 52 ppm and 0.97 ppm, respectively (see example for catalyst B, Fig. 3). The quantification of tetrahedral Al atoms (assumed to be active sites [28]) showed that a similar amount of tetrahedral sites existed in the base samples B and Q (not subjected to hydrothermal treatment), that was significantly higher than that in the treated samples; the decrease in the number of tetrahedral sites was larger in the sample B(TH) that did not incorporate chitosan (see Table 2).

The comparison of the properties of catalysts prepared with and without the incorporation of chitosan shows that the hydrothermal

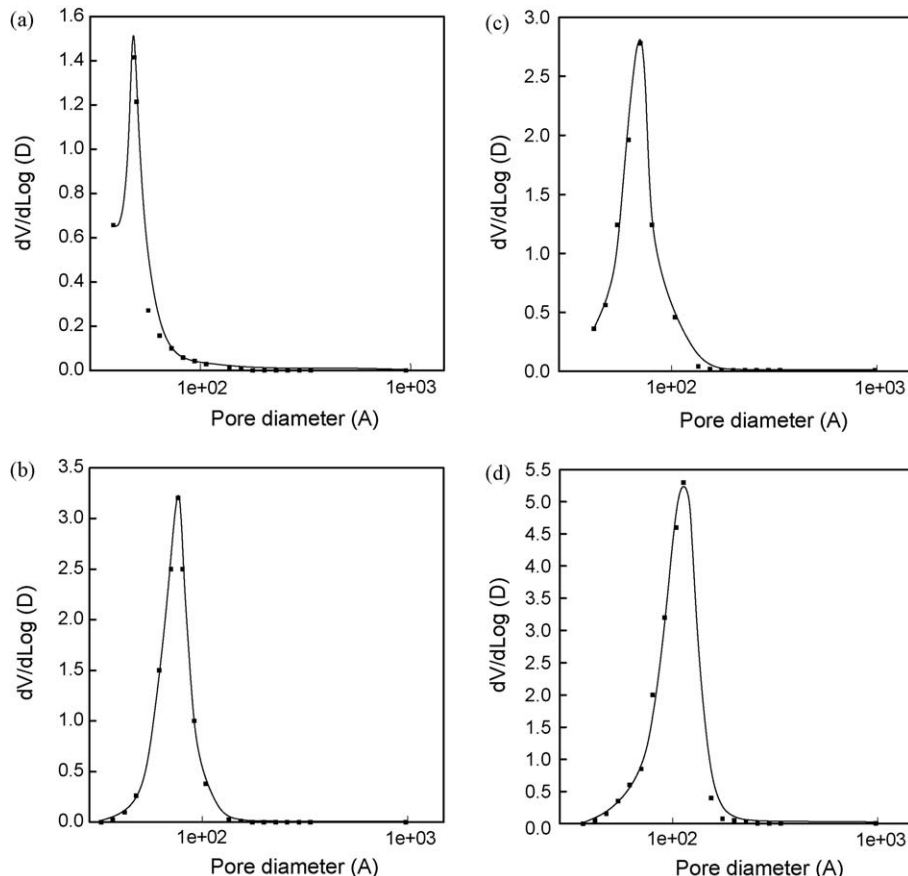


Fig. 1. Pore size distributions of the different silica-aluminas. Catalysts: (a) B, (b) B(TH), (c) Q, (d) Q(TH).

Table 2
Acidic properties of the silica-aluminas.

Catalyst	E_0 (mV) ^a	Acidity (meq/g)	Brönsted/Lewis acid sites ^b	Tetrahedral Al atoms (meq/g)	Tetrahedral/Octahedral Al atoms
B	308	3.5	0.23	2.7	3.6
B(TH)	110	2.6	0.17	1.1	0.7
Q	188	3.0	0.20	2.6	6.0
Q(TH)	159	2.3	0.13	1.9	5.3

^a First reading in the potentiometric titration.

^b From the intensity of the corresponding peaks in the adsorbed pyridine FTIR spectra.

treatment impacted more severely on the reference sample B, without chitosan. This implies that chitosan plays a role in stabilizing the physical properties of the resulting silica-aluminas, also reflecting on some chemical properties, like those evidenced by a higher preservation of the tetrahedral Al sites and of the acid strength.

The TIPB conversion experiments showed that for all the catalysts the conversion increased steadily as a function of the reaction time, and indicated that the activities are different for each sample. The main products were propylene, benzene, isopropylbenzene, di-isopropylbenzene and an isomer of the reactant (C9Bz). The product distributions and yield evolutions were qualitatively the same on all the catalysts. It must be noticed that the same products were observed on equilibrium FCC catalysts [29]. The amount of coke on the different catalysts at the highest reaction time was small, averaging less than 0.5%. Fig. 4 shows the activity profiles and Fig. 5 the typical yield curves. It can be seen that the activity of the reference catalyst B is higher than that of the analogous sample prepared with chitosan. This difference in activity can be correlated with the particular acidic properties. In effect, it can be seen that even though catalyst B has a somewhat higher total amount of acid sites than catalyst Q (particularly Brönsted sites that may have a more important role in this reaction), the acid strength as indicated by the potentiometric analysis is significantly higher (308 mV against 188 mV, respectively).

The catalyst with chitosan that was treated hydrothermally during the preparation (Q(TH)) exhibited a much higher activity than the corresponding reference sample B(TH). Also in this case,

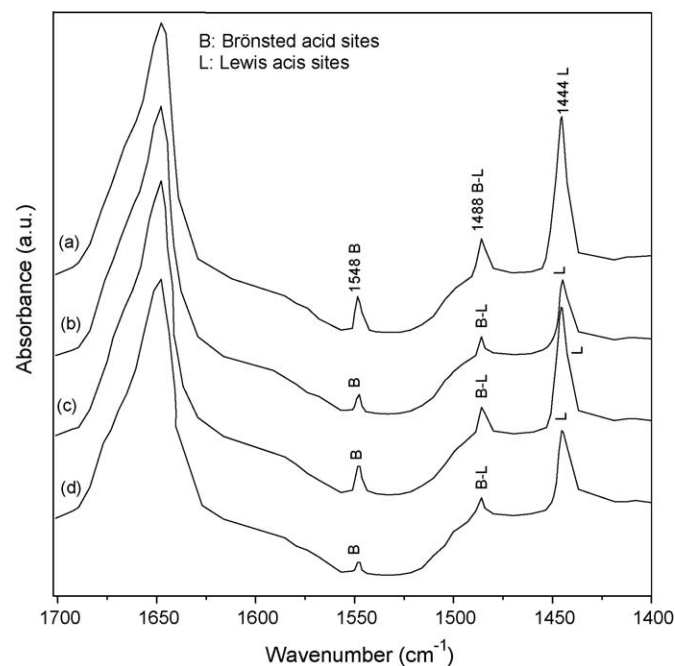


Fig. 2. FTIR spectra of pyridine-sorbed on the different silica-aluminas. Catalysts: (a) B, (b) B(TH), (c) Q, (d) Q(TH).

even though the total amount of acid sites in the B(TH) catalyst is slightly higher, the acid strength of the acid sites in catalyst Q(TH) is higher. Moreover, the relationship between tetrahedral and octahedral aluminium sites is the highest.

The average pore size of these catalysts seems not to have a significant effect on their catalytic performance in the conversion of TIPB. Concerning the property of accessibility, which is crucial in resid cracking, the Akzo accessibility index (AAI) was developed to characterize FCC catalysts, based on a test that measures the liquid phase diffusion of large molecules (asphaltenes) into the catalyst by means of an UV spectrometer, by tracking the relative concentration of the molecules that adsorb at certain wavelength as a function of time [30]. It can explain some facts of the catalytic performances of commercial catalysts; for example, a higher accessibility would ensure a better performance in terms of higher gasoline yields and conversions and lower slurry yields. However, the experimental conditions used are far from those of the commercial process and the AAI observed in amorphous mesopores alumina matrices were from 29 to 45 [29], that is, very close or above the upper limit of applicability of the method (approximately 36).

If these materials are intended to be used in the FCC process, the diffusion of much larger molecules could be hindered according to the pore sizes. It was reported, based on empirical observations, that the matrix in a resid FCC catalyst should have a mixture of mesopores (about 60 Å mean pore size) and macropores (about 200–400 Å mean pore size) [31]. In the case of pure aluminas, the conversion of TIPB showed a direct relationship between accessibility expressed by the AAI index and activity expressed by the value of the constant k_{TIPB} from a simple model representing the direct conversion of TIPB to products without catalyst deactivation [29]. The values of the constants assessed through

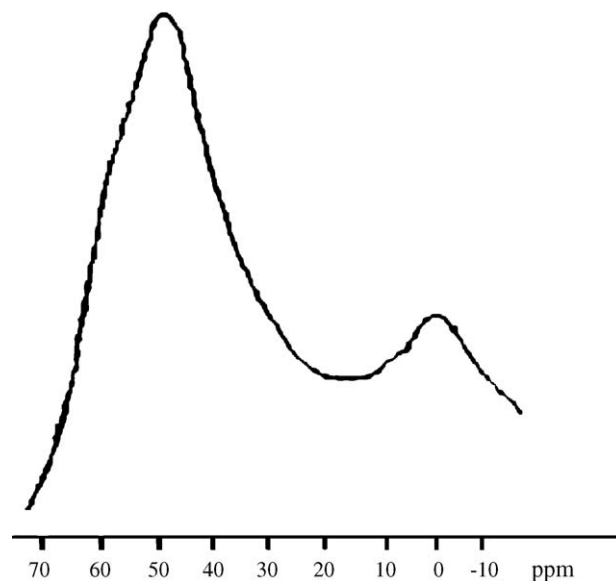


Fig. 3. ²⁷Al MAS-NMR spectrum of catalyst B showing peaks corresponding to 4- (52 ppm) and 6-coordinated (0.97 ppm) Al atoms.

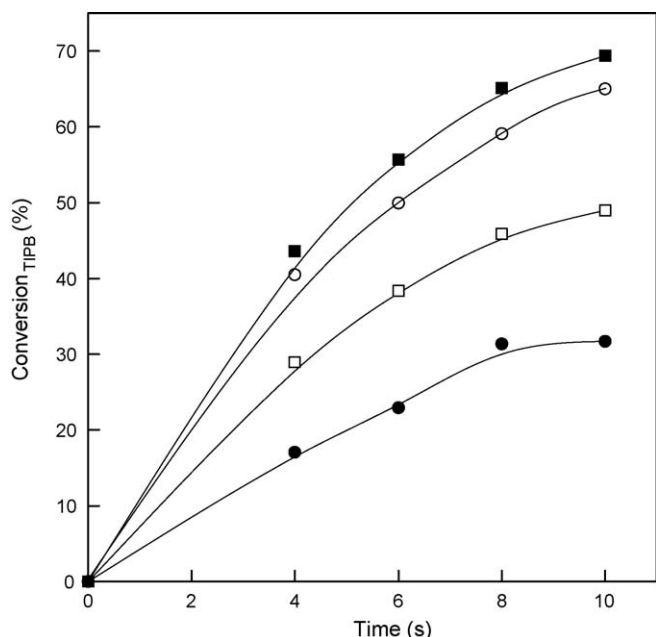


Fig. 4. Conversion of TIPB as a function of reaction time for the various silica-alumina catalysts. Temperature: 400 °C. Symbols: (○) B, (□) B(TH), (●) Q, (■) Q(TH).

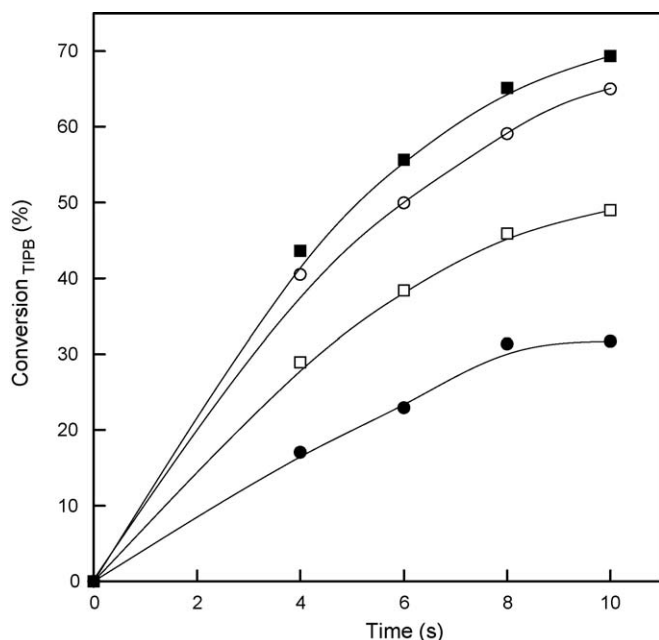


Fig. 5. Yield curves in the conversion of TIPB. Temperature: 400 °C. Catalyst B(TH). Symbols: (■) Di-isopropylbenzene, (●) Propylene, (▲) Isopropylbenzene, (▼) Isomer (C9Bz); (□) Benzene.

a conventional least-square optimization method are shown in Table 3. These values reflect consistency with the previous observations, and show an activity level in these catalysts that is about one order of magnitude larger than that of alumina matrices in commercial FCC catalysts. However, these silica-alumina catalysts are still much less active than the zeolite component in equilibrium FCC catalysts [29]. According to this approach, the catalyst Q(TH) would have the highest accessibility.

Intermolecular hydrogen transfer reactions play a key role in FCC, where they impact product distributions, and many indexes

Table 3

Activity in the conversion of TIPB and i_{TH} from the conversion of CYC6=.

Catalyst	$10^3 k$ (cm ³ /g s)	i_{TH}
B	27.5	0.540
B(TH)	17.7	0.391
Q	10.0	0.612
Q(TH)	30.8	0.442

have been defined in order to evaluate their relative importance. An index can be defined from the results of the conversion of CYC6= that considers the whole set of reactions in the cracking of this cyclic olefinic hydrocarbon [32]. Fig. 6 shows the CYC6= conversion profiles as a function of reaction time. It is observed that the catalysts prepared with the hydrothermal treatment step are somewhat less active than those that were not treated. The most important products of CYC6= conversion were methylcyclopentane (MCPA), methylcyclopentenes (MCPE), cyclohexane (CHA), compounds with twelve carbon atoms per molecule (C12 dimeric products, DIM), and minor amounts of hydrocarbons with six or less carbon atoms per molecule (C6-) and methylcyclohexane (MCHA). The amount of coke on the catalysts averaged 1.2% at the longest reaction time.

It has been shown that the index i_{TH} can be calculated as the slope of the yield of MCPA, a typical product from the hydrogen transfer reactions, as a function of the combined yields of MCPA, MCPE and C6-products, representing hydride transfer, proton transfer and cracking reactions in the system [32]. The corresponding values of the index i_{TH} , that are shown in Table 3, indicate that the hydrogen transfer capacity increases with the number of tetrahedral Al sites in the catalyst surface (refer to Table 2). This is consistent with both the assumption of activity in these sites and the dependency of hydrogen transfer reactions with the density of closely located acidic sites; these sites are referred to as “paired sites” in Y zeolite cracking [18]. The i_{TH} values observed can be considered moderate. It is to be mentioned that the index in equilibrium commercial FCC catalysts ranged from 0.2 to 0.8; values above 0.6 correspond to catalysts with high unit cell sizes above 24.30 Å, with high hydrogen transfer capacity [32].

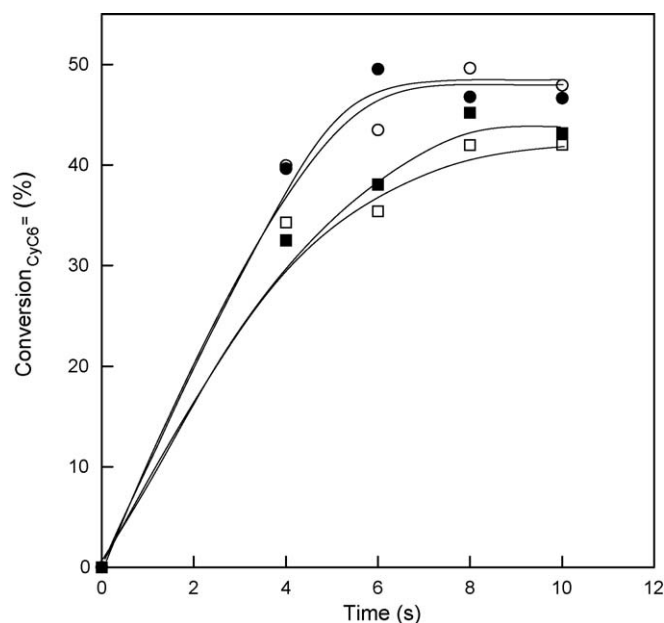


Fig. 6. Conversion of CYC6= as a function of reaction time for the various silica-alumina catalysts. Temperature: 300 °C. Symbols as in Fig. 4.

4. Conclusions

It was possible to synthesise mesoporous amorphous silica-aluminas by means of the addition of the biopolymer chitosan in inorganic–organic networks. The resulting silica-aluminas showed physical properties typical of those materials and controlled, sharp pore size distributions. Chitosan showed to have a stabilizing effect on the physical properties, and also generated a larger relationship of tetrahedral to octahedral aluminium sites in the silica-aluminas. The catalyst with chitosan that was previously subjected to a hydrothermal treatment showed the highest activity in the conversion of tri-isopropylbenzene among the various samples, which could be associated to high accessibility. Its average pore size (100 Å) was the highest. The hydrogen transfer properties as measured with the i_{TH} index from the conversion of cyclohexene revealed to be moderate, as compared to equilibrium commercial FCC catalysts. The catalysts' properties suggest that they could be used as matrices in commercial FCC catalysts.

Acknowledgments

This work was performed with the financial assistance of University of Litoral (Santa Fe, Argentina), Secretary of Science and Technology, Proj. CAID 2005 #01-07; CONICET, PIP 6285/05 and the National Agency for Scientific and Technological Promotion, PICT2005 14-32930.

References

- [1] R.H. Harding, A.W. Peters, J.R.D. Nee, *Appl. Catal. A: Gen.* 221 (2001) 389–396.
 [2] A. Maglio, C.F. Keweshan, R.J. Madon, J.B. McLean, in: *Proceedings of the NPRA Annual Meeting San Antonio, Texas, USA, March 20–22, 1994* (Paper AM-94-59).

- [3] R. Von Ballmoos, C.T. Hayward, *Stud. Surf. Sci. Catal.* 65 (1991) 171–183.
 [4] C. Marcilly, *Arabian J. Sci. Eng.* 21 (2) (1996) 297–312.
 [5] P. O'Connor, S.J. Yanik, *Stud. Surf. Sci. Catal.* 100 (1996) 323–337.
 [6] P. Andreu, *Catal. Lett.* 22 (1993) 135–146.
 [7] N. Hosseinpour, Y. Mortazavi, A. Bazyari, A.A. Khodadadia, *Fuel Process. Technol.* 90 (2009) 171–179.
 [8] N. Kubicek, F. Vaudry, B.H. Chiche, P. Hudec, F. Di Renzo, P. Schulz, F. Fajula, *Appl. Catal. A: Gen.* 175 (1998) 159–171.
 [9] A.N. Shigapov, G.W. Graham, R.W. McCaber, H.K. Plummer, *Appl. Catal. A: Gen.* 210 (2001) 287–300.
 [10] F. Iskandar, K. Mikrajuddin, Okuyama, *Nano Lett.* 1 (5) (2001) 231–234.
 [11] Z. Kónya, V.F. Puentes, I. Kiricsi, J. Zhu, A. Alivisatos, G.A. Somorjai, *Nano Lett.* 2 (8) (2002) 907–910.
 [12] A. Hidrobo, J. Retuert, P. Araya, J. Porous Mater. 10 (2003) 231–234.
 [13] V. Puchol, J. El Haskouri, J. Latorre, C. Guillem, A. Beltrán, D. Beltrán, P. Amorós, *Chem. Commun.* 19 (2009) 2694–2696.
 [14] J. Retuert, R. Quijada, V. Arias, *Chem. Mater.* 10 (1998) 3923–3927.
 [15] J. Retuert, R. Quijada, V. Arias, M. Yazdani-Pedram, *J. Mater. Res.* 18 (2003) 487–494.
 [16] H.V. Fajardo, A.O. Martins, R.M. de Almeida, L.K. Noda, L.F.D. Probst, N.L.V. Carreño, A. Valentini, *Mater. Lett.* 59 (2005) 3963–3967.
 [17] W.S. Letzsch, A.G. Ashton, *Stud. Surf. Sci. Catal.* 76 (1993) 441–498.
 [18] U. Sedran, *Catal. Rev. Sci. Eng.* 36 (1994) 405–431.
 [19] E.F.S. Aguiar, M.L.M. Valle, M.P. Silva, D.F. Silva, *Zeolites* 15 (1995) 620–623.
 [20] Cumming, Wojchiechowsky, *Catal. Rev. Sci. Eng.* 38 (1996) 101–157.
 [21] R. Cid, G. Pecchi, *Appl. Catal.* 14 (1985) 15–21.
 [22] de Lasa, H.I. U.S. Patent 5,102,628.(1992).
 [23] F.J. Passamonti, G. de la Puente, U.A. Sedran, *Ind. Eng. Chem. Res.* 43 (2004) 1405–1410.
 [24] S. Al-Khattaf, *Ind. Eng. Chem. Res.* 46 (2007) 59–69.
 [25] A. Rahman, G. Lemay, A. Adnot, S. Kaliaguine, *J. Catal.* 112 (1988) 453–463.
 [26] J.E. Mapes, R.P. Eischens, *J. Phys. Chem.* 58 (1954) 1059.
 [27] N.W. Cant, L.H. Little, *Nature* 211 (1966) 69–70.
 [28] W.O. Haag, R.M. Lago, P.B. Weisz, *Nature* 309 (1984) 589–591.
 [29] M. Falco, E. Morgado, N. Amadeo, U. Sedran, *Appl. Catal. A: Gen.* 315 (2006) 29–34.
 [30] A.K. Hakuli, P. Imhof, C.W. Kuehler, in: *Proceedings of the Akzo Nobel ECO-MAGIC Symposium, Noordwijk, The Netherlands, June 10–13, (2001)*, p. F-4.
 [31] J.S. Magee, W.S. Letzsch, in: *Proceedings of the ACS Symposium Series, ACS, Washington, USA, Fluid catalytic cracking III, (1994)*, pp. 349–371, Chap. 25.
 [32] G. de la Puente, U. Sedran, *Chem. Eng. Sci.* 55 (2000) 759–765.